

Transport Properties of Ca-doped γ -Na_xCoO₂

Yasuhiro ONO, Nobuhiko KATO, Yuzuru MIYAZAKI and Tsuyoshi KAJITANI

Department of Applied Physics, Graduate School of Engineering, Tohoku University, Sendai 980-8579, Japan

Single-phase polycrystalline samples of γ -Na_{0.70}Ca_xCoO_{2- δ} are successfully synthesized in the concentration range, $0 \leq x \leq 0.07$, by a two-step sintering procedure, i.e., γ -Na_{0.70}CoO₂ powder mixed with an appropriate amount of Ca(NO₃)₂·4H₂O is sintered at 873 K and 1123 K in air for 12 h. ICP analysis data indicate that Na content (Na/Co = 0.64–0.67) is slightly lower than the nominal one (0.70). Oxygen deficiency is determined by the automated iodometric titration technique ($\delta = 0.025$ –0.033). In this system, formal valence of Co ion linearly decreases from +3.27(2) at $x=0$ to +3.16(2) at $x=0.07$, implying electron doping. We have studied thermoelectric properties of γ -Na_{0.70}Ca_xCoO_{2- δ} at high temperature. Both electrical resistivity, ρ , and Seebeck coefficient, S , almost linearly increase with increasing temperature. The largest power factor, $S^2/\rho = 6.4 \times 10^{-4} \text{ W m}^{-1} \text{ K}^{-2}$ at 985 K, is obtained for the sample with $x=0.0175$.

[Received July 28, 2003; Accepted December 10, 2003]

Key-words: Thermoelectric material, Layered oxide, γ -Na_xCoO₂, Ca-doping

1. Introduction

Recent discovery of potential oxide thermoelectric (TE) materials has attracted much attention, since high temperature applications such as power generation utilizing waste heat from factories and engines can be expected for these materials.¹⁻⁴⁾ The layered cobaltite, γ -Na_xCoO_{2- δ} , is one of the most promising p-type TE materials and exhibits high Seebeck coefficient ($S = 200 \mu\text{V K}^{-1}$), low electrical resistivity ($\rho = 5.2 \mu\Omega \text{ m}$) and low thermal conductivity ($\kappa = 5.1 \text{ W m}^{-1} \text{ K}^{-1}$) at $T = 800 \text{ K}$.⁵⁾ The dimensionless figure of merit, $ZT = S^2T/\rho\kappa$, for a single crystal of γ -Na_xCoO_{2- δ} becomes 1.2 at this temperature, which satisfies the empirical criterion for practical applications ($ZT \geq 1$). Despite of high carrier density (10^{27} – 10^{28} m^{-3}), the Seebeck coefficient of γ -Na_xCoO_{2- δ} is unusually high. It is difficult to understand such high Seebeck coefficient within the framework of a conventional band picture.

The substitution effects of Li, Ag, Mg, Ca, Sr, Ba and La for Na in polycrystalline γ -Na_xCoO_{2- δ} have been systematically studied by Yakabe et al.,⁶⁾ Fujita et al.,⁷⁾ Kawata et al.⁸⁾ and Ishikawa et al.⁹⁾ Kawata et al.⁸⁾ reported that the Seebeck coefficient, S , appreciably increases with increasing x in γ -Na_{0.55-x}Ca_xCoO₂. Unfortunately, the electrical resistivity, ρ , was so high that the TE performance was not improved markedly.⁸⁾ Recently, we found that Ca can be introduced into the highly vacant Na sheet of γ -Na_xCoO₂ without changing Na content remarkably (Na/Co = 0.64–0.67). In this paper, synthesis, chemical analyses and transport properties of γ -Na_{0.70}Ca_xCoO_{2- δ} are presented.

2. Experimental

Polycrystalline samples of γ -Na_{0.70}CoO₂ were prepared from Na₂CO₃ (99.5%) and Co₃O₄ (99.9%) by a conventional solid-state reaction, as described in the previous report.¹⁰⁾ The Ca-doped polycrystalline samples, γ -Na_{0.70}Ca_xCoO_{2- δ} ($x = 0.0175, 0.035, 0.07, 0.105$ and 0.175), were prepared by the following two-step sintering procedure. The starting materials, γ -Na_{0.70}CoO₂ and Ca(NO₃)₂·4H₂O (99.9%), were thoroughly mixed, sintered at 873 K for 12 h in air and subsequently homogenized at 1123 K for 12 h in air with an intermediate grinding. Powder X-ray diffraction intensities of these samples were measured using a RIGAKU RAD-X diffractometer (CuK α) equipped with a curved-graphite monochromator, which is needed to remove fluorescent X-ray

of Co ion. Na, Ca and Co contents in the samples were determined by the inductively coupled plasma (ICP) analysis. The valence of Co ion and the oxygen deficiency were chemically evaluated by a standard iodometric titration technique using an auto buret AUT-501 (TOA DKK), which was operated in Ar atmosphere to avoid the oxidation of Co ion. The electrical resistivity and the Seebeck coefficient were measured in the temperature range from 480 K to 985 K using an automated Seebeck coefficient measuring apparatus, Ozawa RZ2001i.

3. Results and discussion

3.1 Powder X-ray diffraction

Figure 1 shows the observed powder X-ray diffraction patterns. A few impurity peaks marked by closed circles were observed for the samples with $x=0.105$ and 0.175 . The second phase in these heavily Ca-doped samples was identified as CaO. Except for those impurity peaks, the diffraction patterns of the Ca-doped samples are almost the same as that of γ -Na_{0.70}CoO₂ ($x=0$). **Figure 2** shows the crystal structure of γ -Na_{0.70}CoO₂.¹⁰⁾ There are many vacant sites in Na⁺ layer and it is likely to introduce other ions to these sites. Since the ionic radius of Ca²⁺ (0.100 nm) is similar to that of Na⁺ (0.102 nm),¹¹⁾ the doped Ca²⁺ can easily occupy the vacant Na⁺ site. Lattice parameters of the present samples were determined by the least-squares calculation from the 2θ values of well-de-

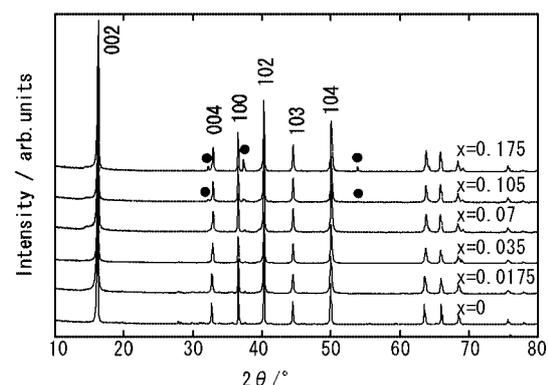


Fig. 1. Powder X-ray diffraction patterns of γ -Na_{0.70}Ca_xCoO_{2- δ} . Closed circles indicate the impurity peaks (CaO).

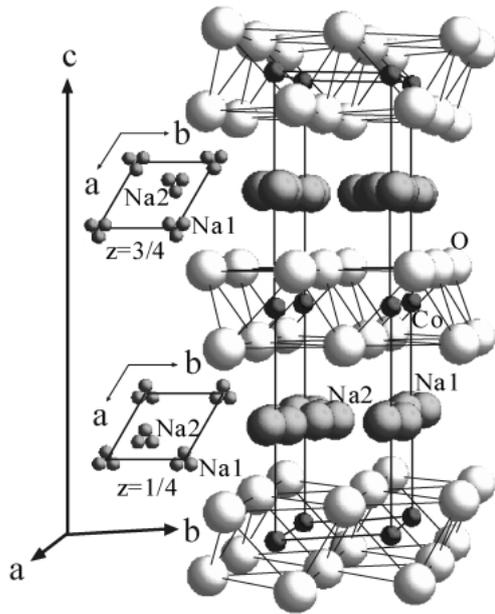


Fig. 2. Crystal structure of $\gamma\text{-Na}_{0.70}\text{CoO}_2$. Possible sites in Na sheets at $z=1/4$ and $3/4$ are schematically represented. Na(1) and Na(2) ions are statistically distributed over three equivalent positions, respectively. Their sites are not fully occupied with Na^+ .

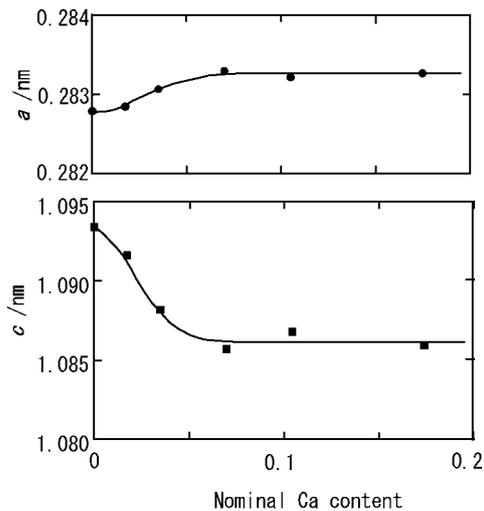


Fig. 3. Lattice parameters (a and c) vs. nominal Ca content in $\gamma\text{-Na}_{0.70}\text{Ca}_x\text{CoO}_{2-\delta}$ system.

finer Bragg reflections. **Figure 3** shows the lattice parameters, a and c , as a function of the nominal Ca content, where their error-bars are inside the symbols. In $0 \leq x \leq 0.07$, the lattice parameter, a , slightly increases with increasing x , while the lattice parameter, c , shows relatively large decrease. Above $x=0.07$, both a and c remain almost constant. This change corresponds to the appearance of the second phase in Fig. 1. X-ray diffraction analysis indicates that the single-phase $\gamma\text{-Na}_{0.70}\text{Ca}_x\text{CoO}_{2-\delta}$ is successfully synthesized in the range, $0 \leq x \leq 0.07$.

3.2 Chemical analysis

The nominal and analyzed chemical compositions of the present samples are listed in **Table 1**. The analyzed Na content (0.63–0.67) is slightly lower than the nominal one (0.70) due

Table 1. Chemical Compositions of $\gamma\text{-Na}_{0.70}\text{Ca}_x\text{CoO}_{2-\delta}$

x	Na	Ca	Co	δ
0	0.67	0	1	0.031 ± 0.003
0.0175	0.66	0.02	1	0.033 ± 0.002
0.035	0.65	0.04	1	0.028 ± 0.004
0.07	0.64	0.08	1	0.025 ± 0.002
0.105	0.63	0.11	1	-0.005 ± 0.003
0.175	0.63	0.16	1	-

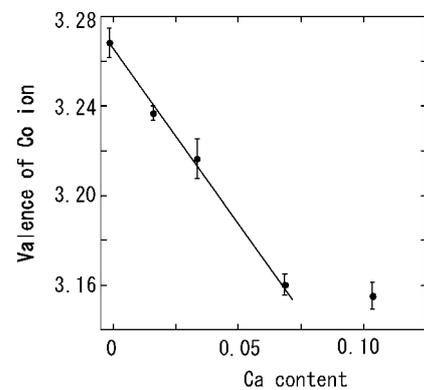


Fig. 4. Valence of Co ion vs. Ca content in $\gamma\text{-Na}_{0.70}\text{Ca}_x\text{CoO}_{2-\delta}$ system.

to the evaporation of Na during the sintering.¹²⁾ On the other hand, there are good agreements between the nominal and analyzed Ca contents. The sum of Na and Ca contents in the single-phase samples is lower than 0.74, which is the upper limit of Na content in $\gamma\text{-Na}_x\text{CoO}_2$.¹³⁾ The oxygen deficiency determined by the titration measurement is negligibly small ($\delta = 0.025\text{--}0.033$) in the single-phase region. **Figure 4** shows the valence of Co ion versus Ca content, x . In the single-phase region, the valence of Co ion linearly decreases from +3.27(2) at $x=0$ to +3.16(2) at $x=0.07$, implying electron doping. These fractional values are due to the coexistence of Co^{3+} and Co^{4+} ,^{10),14)} i.e., the mixed valence state of Co ion.

3.3 Transport properties

Figure 5(a) shows temperature variation of the electrical resistivity, ρ , for $\gamma\text{-Na}_{0.70}\text{Ca}_x\text{CoO}_{2-\delta}$. The ρ value increases with increasing Ca content, x . The major carrier of the sample with $x=0$ is the electron hole and the population of holes decreases with increasing x .⁸⁾ Accordingly, the increase in ρ is explained by the decrease of hole carriers. But, the high ρ values of the samples with $x=0.105$ and 0.175 partly come from the insulating second-phase, CaO.

Figure 5(b) shows temperature variation of the Seebeck coefficient, S . Enhancement of S by the Ca-doping is clearly observed. For the single-phase samples, the S value tends to increase with increasing x . But, the S values of the sample with $x=0.0175$ are almost at the same level as those of the sample with $x=0.035$. **Figure 6** shows temperature variation of power factor, (S^2/ρ) . The maximum power factor, $6.4 \times 10^{-4} \text{ W m}^{-1} \text{ K}^{-2}$ at 985 K, is obtained for this sample ($x=0.0175$) because the ρ values are as low as those of the sample with $x=0$.

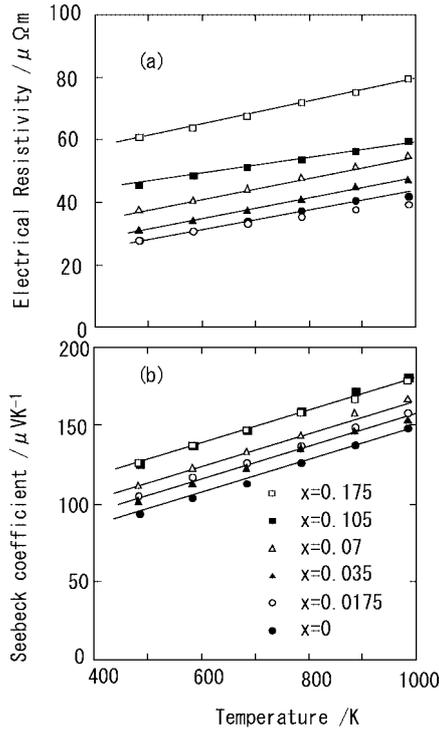


Fig. 5. Temperature variations of electrical resistivity (a) and Seebeck coefficient (b) of γ - $\text{Na}_{0.70}\text{Ca}_x\text{CoO}_{2-\delta}$.

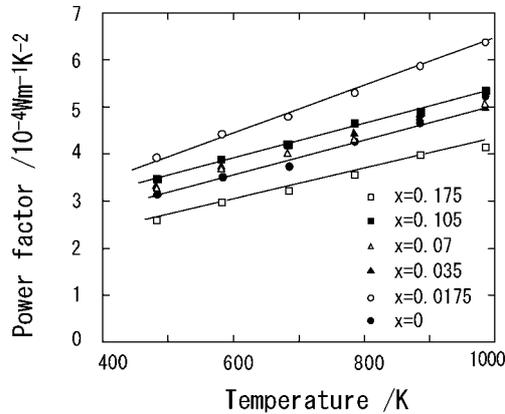


Fig. 6. Temperature variations of power factor of γ - $\text{Na}_{0.70}\text{Ca}_x\text{CoO}_{2-\delta}$.

The largest power factor is about 1.3 times larger than that of the end member γ - $\text{Na}_{0.70}\text{CoO}_2$ ($x=0$) in the present results.

4. Conclusion

The single-phase polycrystalline samples of γ - $\text{Na}_{0.70}\text{Ca}_x\text{CoO}_{2-\delta}$ with the negligible oxygen deficiency ($\delta=0.025$ – 0.033) were successfully synthesized in the range, $0 \leq x \leq 0.07$. The valence of Co ion linearly decreases from $+3.27$ (2) at $x=0$ to $+3.16$ (2) at $x=0.07$. Both the electrical resistivity and Seebeck coefficient tend to increase with increasing Ca content, x . The largest power factor was obtained at $x=0.0175$. The Ca-doping is an effective method to improve the TE performance of γ - $\text{Na}_{0.70}\text{CoO}_{2-\delta}$.

Acknowledgement This research was partly supported by CREST (Core Research for Evolution Science and Technology) project of JST (Japan Science and Technology Corporation).

References

- 1) Terasaki, I., Sasago, Y. and Uchinokura, K., *Phys. Rev.*, Vol. B56, pp. R12685–R12687 (1997).
- 2) Yasukawa, M. and Murayama, N., *Mater. Sci. Eng.*, Vol. B54, pp. 64–69 (1998).
- 3) Funahashi, R., Matsubara, I. and Sodeoka, S., *Appl. Phys. Lett.*, Vol. 76, pp. 2385–2387 (2000).
- 4) Miyazaki, Y., Kudo, K., Akoshima, M., Ono, Y., Koike, Y. and Kajitani, T., *Jpn. J. Appl. Phys.*, Vol. 40, pp. L531–L534 (2001).
- 5) Fujita, K., Mochida, T. and Nakamura, K., *Jpn. J. Appl. Phys.*, Vol. 40, pp. 4644–4647 (2001).
- 6) Yakabe, H., Fujita, K., Nakamura, K. and Kikuchi, K., Proc. 17th International Conference on Thermoelectrics, pp. 551–558 (1998).
- 7) Fujita, K., Nakamura, K. and Yamashita, S., Proc. 18th International Conference on Thermoelectrics, pp. 481–484 (1999).
- 8) Kawata, T., Iguchi, Y., Itoh, T., Takahata, K. and Terasaki, I., *Phys. Rev.*, Vol. B60, pp. 10584–10587 (1999).
- 9) Ishikawa, R., Ono, Y., Miyazaki, Y. and Kajitani, T., *Jpn. J. Appl. Phys.*, Vol. 41, pp. L337–L339 (2002).
- 10) Ono, Y., Ishikawa, R., Miyazaki, Y. and Kajitani, T., *J. Phys. Soc. Jpn.*, Vol. 70, Suppl. A, pp. 235–238 (2000).
- 11) Shannon, R. D. and Prewitt, C. T., *Acta Cryst.*, Vol. B25, pp. 925–946 (1969).
- 12) Motohashi, T., Naujalis, E., Ueda, R., Isawa, K., Karppinen, M. and Yamauchi, H., *Appl. Phys. Lett.*, Vol. 79, pp. 1480–1482 (2001).
- 13) Delmas, C., Fouassier, C. and Hagenmuller, P., *Physica*, Vol. B99, pp. 81–85 (1980).
- 14) Ray, R., Ghoshray, A., Ghoshray, K. and Nakamura, S., *Phys. Rev.*, Vol. B59, pp. 9454–9461 (1999).